Supporting Information:

Watching Excited State Dynamics with Optical and X-ray Probes: The Excited State Dynamics of Aquocobalamin and Hydroxocobalamin.

Roseanne J. Sension[1,2]*, Taylor P. McClain[3], Ryan M. Lamb[1], Roberto Alonso-Mori[4], Frederico Alves Lima[5], Fernando Ardana-Lamas[5], Mykola Biednov[5], Matthieu Chollet[4], Taewon Chung[1], Aniruddha Deb[1,3], Paul A. Dewan Jr.[3], Leland B. Gee[4], Joel Huang Ze En[1], Yifeng Jiang[5], Dmitry Khakhulin[5], Jianhao Li[1], Lindsay B. Michocki[1], Nicholas A. Miller[1], Florian Otte[5], Yohei Uemura[5], Tim B. van Driel[4], James E Penner-Hahn[1,3]*

[1]Department of Chemistry, University of Michigan, 930 N University Ave. Ann Arbor, Michigan, 481091055, U.S.A.

[2]Department of Physics, University of Michigan, 450 Church Street, Ann Arbor, Michigan, 48109-1040, U.S.A.

[3]Biophysics, University of Michigan, 930 N University Ave. Ann Arbor, Michigan, 48109-1055, U.S.A.

[4]Linac Coherent Light Source, SLAC National Accelerator Laboratory, 2575 Sand Hill Road, Menlo Park, CA 94025, U.S.A.

[5]Femtosecond X-ray Experiments Group, European XFEL, Holzkoppel 4, 22869 Schenefeld, Germany,

*Corresponding Authors e-mail: rsension@umich.edu, Phone: 734-763-6074; jeph@umich.edu

CONTENTS:

Setting Pulse Overlap (t=0) for XANES and XES S3

UV-Visible TA Measurements S3-S5

XANES Excitation Fraction and Polarization Correction S5-S7

HOCbl XAS Pre-Edge Transitions S8

XES Difference Spectra S8

Ground State FDMNES Simulations S9

FDMNES Simulations of the Species at 150 fs (**B**) S10-S13

FDMNES Simulations of Species at t>500 fs (**C**) S14

Influence of Axial Bonds on the Valence-to-Core Emission and Pre-Edge Absorption S15

Representative FDMNES input file S16

Representative ORCA input file S19

Data availability S21

Setting Pulse Overlap (t=0)

The position for temporal overlap of the optical and X-ray pulses was set for each experiment by looking at the earliest changes in the spectrum. While the actual stage position for t=0 could be slightly earlier than this (i.e. at negative times in the plots below), it is no later than this.

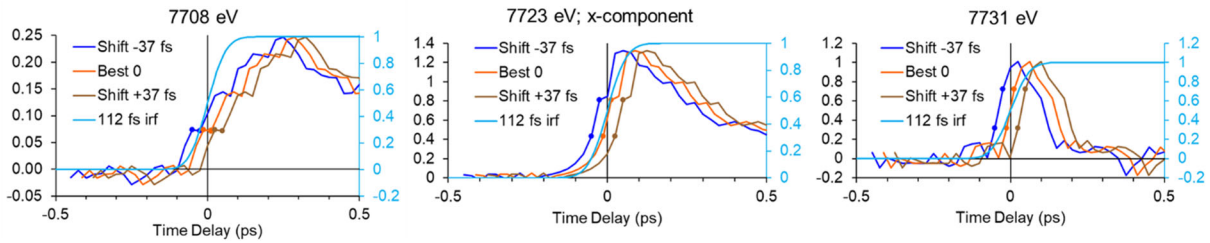

Figure S1. Examination of the earliest transients in the H_2OCbl^+ tr-XANES data to set the zero time-delay point. The time-delay for the HOCbl data is also set using this value.

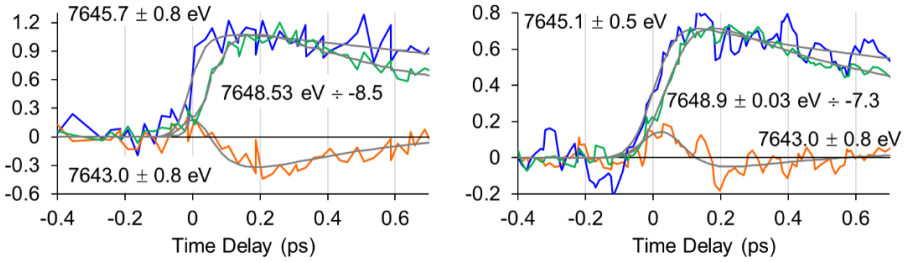

Figure S2. Examination of the earliest transients in the tr-XES data to set the zero time-delay point. Traces are averaged over the indicated energy ranges. If no range is indicated, data is from one energy.

UV-Visible TA Measurements

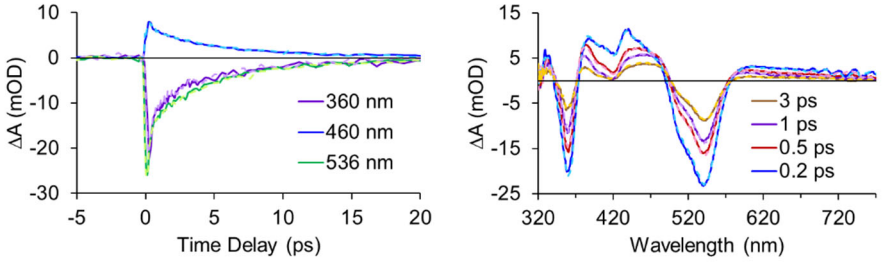

Figure S3. Comparison of transient absorption signals following excitation of HOCbl, pH 10, at 520 nm. The data plotted using solid lines was obtained in 1 M potassium phosphate buffer. The data plotted using dashed lines was obtained for 10 mM potassium phosphate buffer. Both samples were measured on the same day under the same pump and probe conditions.

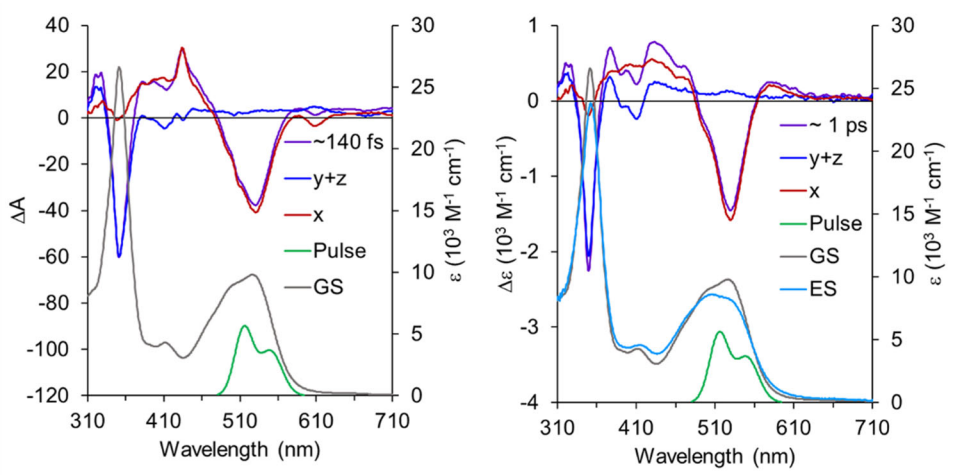

Figure S4. Polarization decomposition for states **B** (~140 fs), left and **C**(~1 ps) of H_2OCbl^+, right, using an excitation pulse centered around 530 nm, covering the range excited in the XANES measurements. The results are similar to those obtained with 562 nm excitation (Figure 11 in the main text).

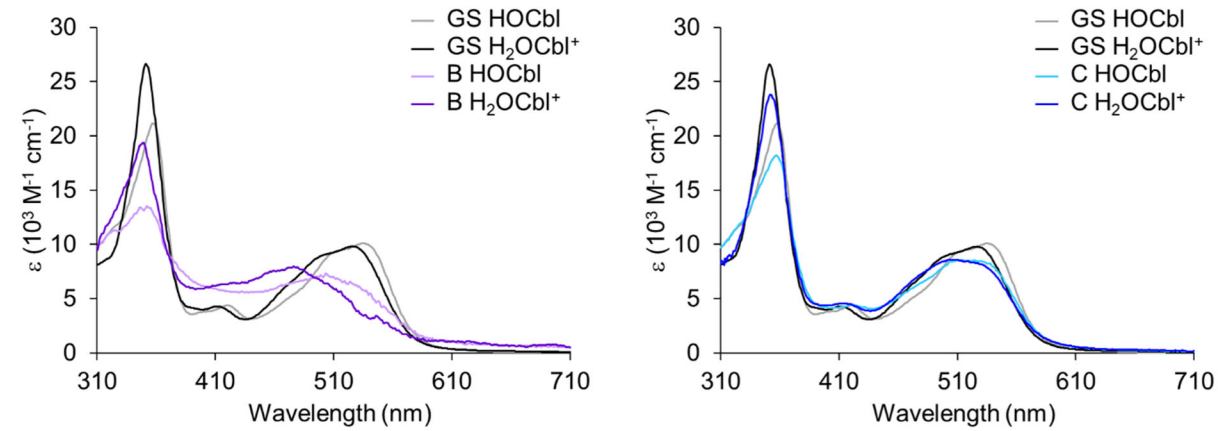

Figure S5. Left: Comparison of the ground state and estimated **B** species spectra for H_2OCbl^+ and HOCbl. Right: Comparison of the ground state and **C** species spectra for H_2OCbl^+ and HOCbl.

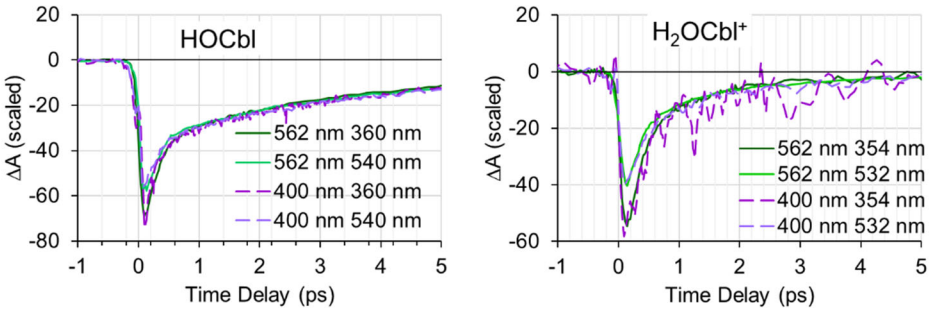

Figure S6. Comparison of isotropic transient kinetics of bleach recovery following excitation at 400 nm and 562 nm. The time scales are independent of excitation wavelength.

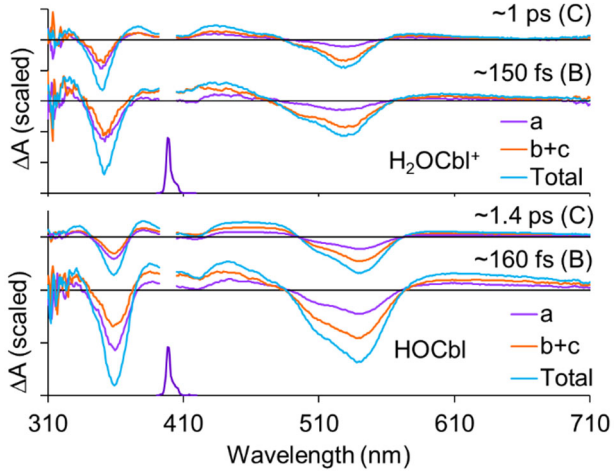

Figure S7. Polarization resolved difference spectra following excitation of H_2OCbl^+ and HOCbl at ca. 400 nm. The pulse spectrum is plotted in the figure. The component parallel to the average transition dipole direction excited at 400 nm is designated "a" and the sum of the two perpendicular directions is designated "b+c".

XANES Excitation Fraction and Polarization Correction

The excitation fraction for H_2OCbl^+ in the first measurement was estimated at 0.25 as described earlier for MeCbl. Both H_2OCbl^+ and MeCbl were of similar concentration and data were obtained under similar conditions. The polarization discrimination for MeCbl was good, as evidenced by the absence of a pre-edge bleach in the x component. In addition, the polarization

discrimination is good in a measurement of propylcobalamin obtained immediately before the measurement on H_2OCbl^+ (see below). Good polarization discrimination is only consistent with an excitation fraction well below 0.33. For the second data set, the laser fluence was higher and we estimate an excitation fraction of 0.4, although it could be as high as 0.5. The estimated spectra for species **B** and **C** for the two measurements are compared in Figure S8.

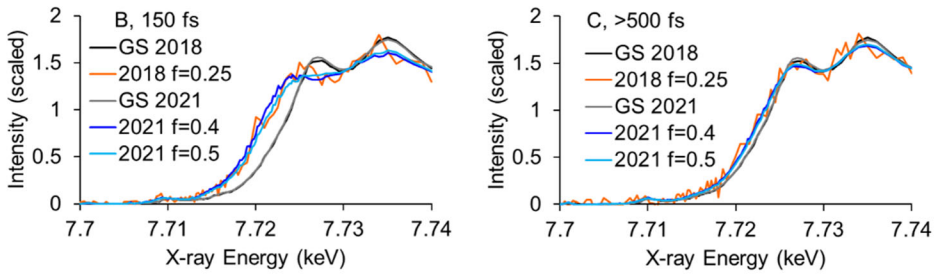

Figure S8. Ground state XANES spectra and estimated excited state spectra for H_2OCbl^+. The excitation fraction is indicated in the legend.

The higher excitation fraction for the data obtained in LW26, 2021 results in a degradation in the polarization discrimination. However, it does not affect the spectral shape of the time-dependent isotropic difference spectra. A polarization correction can be estimated by assuming that the measured "Parallel" spectrum $\Delta A_{\parallel}$ is actually a mixture of parallel and perpendicular contributions and measured "Perpendicular" spectrum $\Delta B_{\perp}$ includes a parallel contribution.

$$\begin{aligned} \Delta A_{\parallel} &= \Delta I_{\parallel} + 2\alpha\Delta I_{\perp} \\ \Delta B_{\perp} &= (1+\alpha)\Delta I_{\perp} + \alpha\Delta I_{\parallel} \end{aligned} \tag{1}$$

The total signal remains as expected: $\Delta A_{\parallel} + 2\Delta B_{\perp} = (1+2\alpha)(\Delta I_{\parallel} + 2\Delta I_{\perp})$. If α=1, then $\Delta A_{\parallel} = \Delta B_{\perp}$, both are equivalent to $\Delta I_{\parallel} + 2\Delta I_{\perp}$, there is no polarization discrimination, and the excitation fraction approaches 1. For values of α<1, the corrections to the directional contributions can be estimated as:

$$\Delta S_x = \left(2\Delta A_{\parallel} - \Delta B_{\perp}\right)\frac{1+\alpha}{1-\alpha} - \left(3\Delta B_{\perp} - \Delta A_{\parallel}\right)\frac{\alpha}{1-\alpha}$$
$$\Delta S_{y+z} = \left(3\Delta B_{\perp} - \Delta A_{\parallel}\right)\frac{1}{1-\alpha} - \left(2\Delta A_{\parallel} - \Delta B_{\perp}\right)\frac{2\alpha}{1-\alpha} \quad (2)$$

The isotropic spectra and polarization decomposition results for measurements on H_2OCbl^+ and propylcobalamin (PrCbl) at 1 ps time delay are compared in Figure S9. A value of α=0 assumes that there is no polarization degradation (not possible for an excitation fraction above 0.33). A value of α=0.25 requires an excitation fraction ≤0.5. If the excitation fraction is larger, the value for α must also be larger.

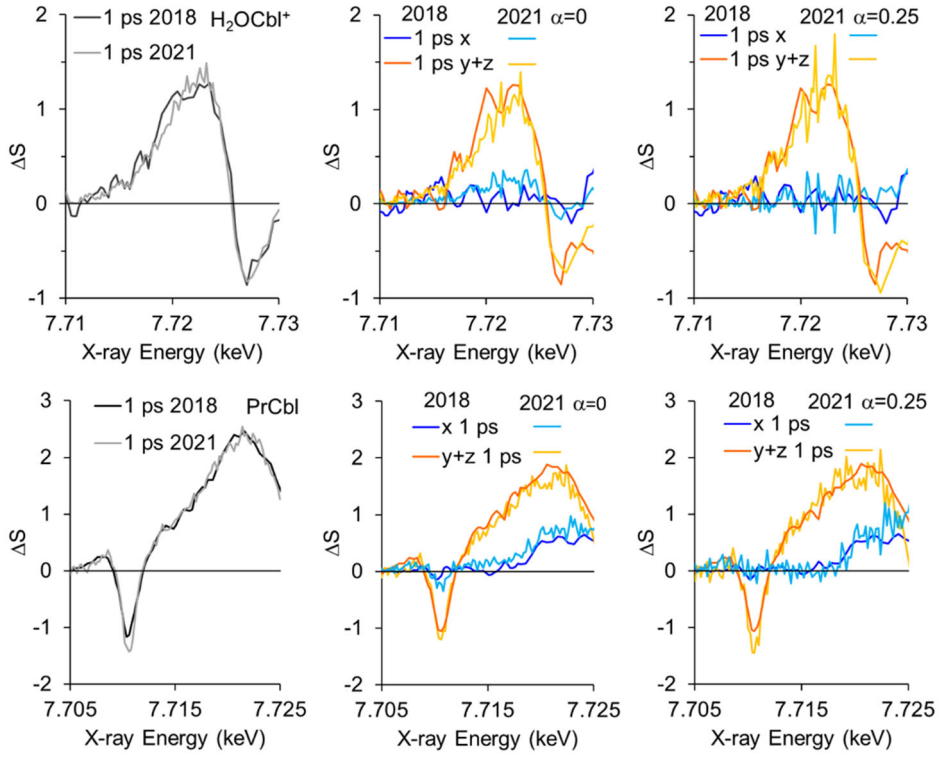

Figure S9. Comparison of the XANES difference signal around 1 ps from measurements in 2018 and 2021. The total signals are scaled and plotted in the left most column for H_2OCbl^+ (top row) and PrCbl (bottom row). The middle column plots the polarization decomposition assuming α=0 for both measurements. The right column compares the 2018 data (α=0) with the 2021 data α=0.25.

XANES Pre-Edge Transitions

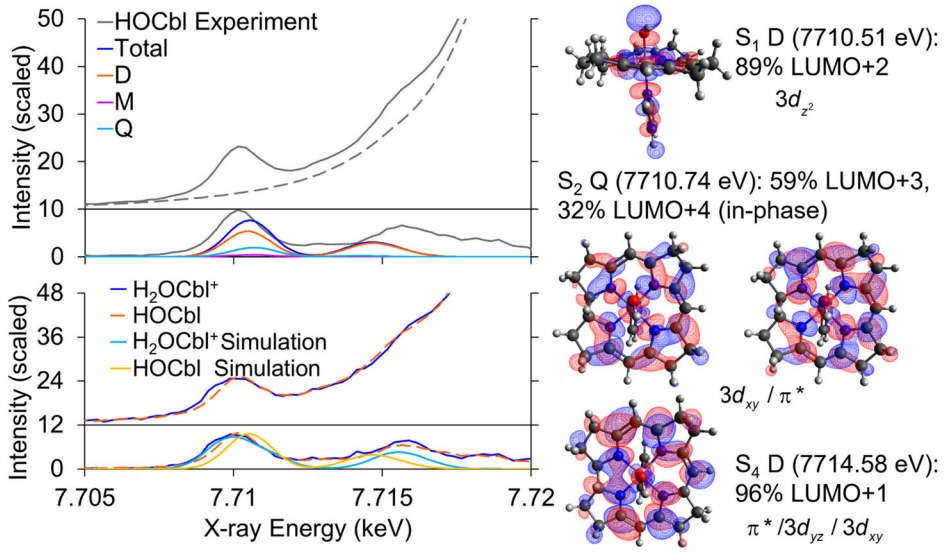

Figure S10. Experimental and simulated pre-edge transitions for HOCbl. The baseline under the pre-edge transitions is estimated and subtracted from the data as shown to allow better comparison with the calculated spectrum. The dominant orbitals contributing to the peaks are shown to the right, The results for HOCbl and H_2OCbl^+ are compared in the lower panel.

XES Difference Spectra

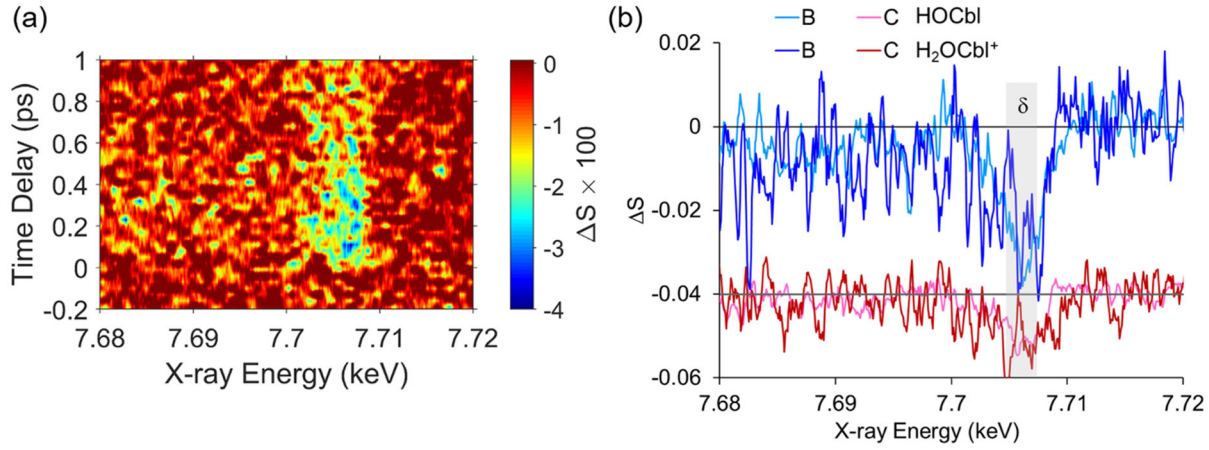

Figure S11. (a) Surface plot of the valence-to-core region for H_2OCbl^+. The data has been smoothed using a 1 eV average, compared with the 0.5 eV average used for HOCbl. (b) Comparison of the species associated XES difference spectra for HOCbl and H_2OCbl^+. The general trends are the same for both molecules.

Ground State FDMNES Simulation

Simulations were performed using the FDMNES program. The ground state structure reported by Kratky et al. was used to model the coring ring. To reduce the computational time and memory requirements, all calculations were performed on structures truncated by replacing all of the peripheral groups with methyl groups, truncating the dimethylbenzimidazole to benzimidazole, and ensuring that all C-H bond lengths were reasonable (ca. 1.09 Å).

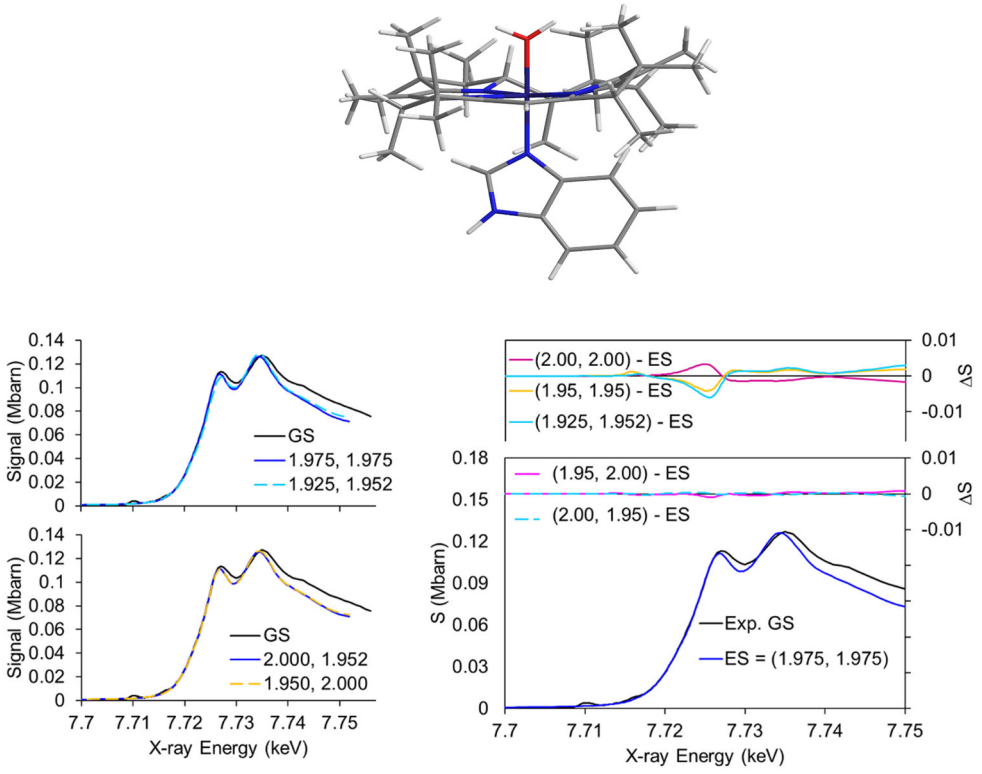

Figure S12. Comparison of the ground state XANES spectrum of H_2OCbl^+ with FDMNES simulations for the truncated structure illustrated with axial bond lengths as indicated in the legends (Co-N_{DMB}, Co-O in Å). The plot on the top left compares simulations with the crystal structure bond lengths of (1.925 Å, 1.952 Å) and with somewhat longer bonds (1.975 Å, 1.975 Å). The plot on the bottom left compares simulations using (2.000 Å, 1.952 Å) and (1.950 Å, 2.000 Å) with the experimental spectrum. The plots on the right compare the differences between a simulation using (1.975 Å, 1.975 Å) and other pairs of axial bond lengths. For a total axial distance of 3.95 Å, the simulations are essentially identical.

FDMNES Simulations of the Species at 150 fs (B)

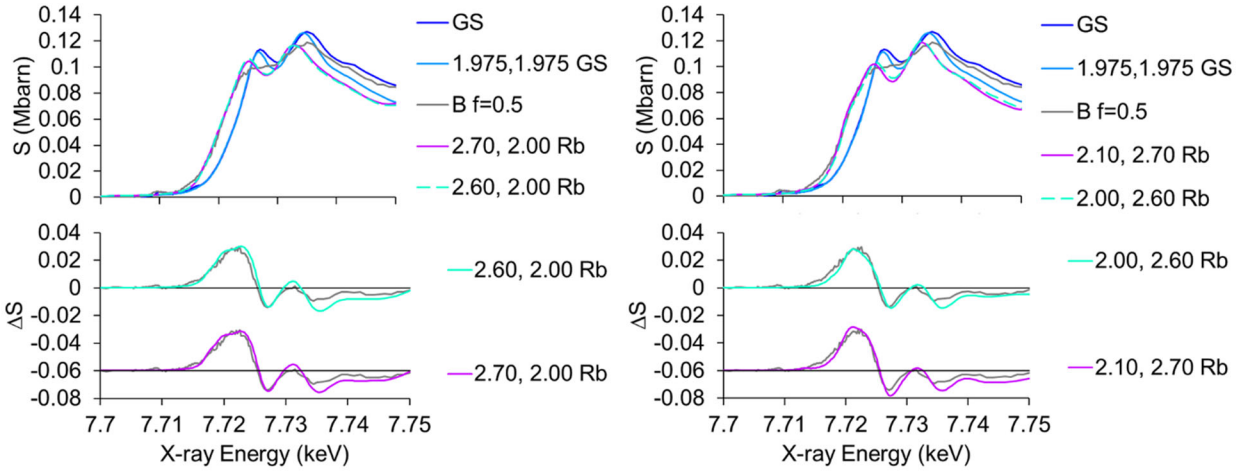

Figure S13. Comparison for H_2OCbl^+ of simulated and experimental XANES spectra for the species **B**, present at 150 fs as in Figure 14, but now comparing with an excitation fraction of f=0.5.

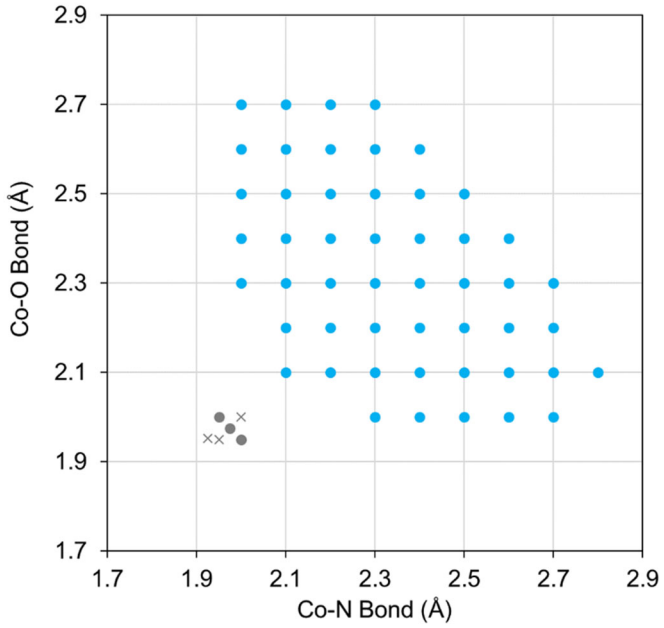

Figure S14. FDMNES simulations were performed for the axial bond lengths as indicated in blue on this grid. The ground state bond lengths most consistent with the measured XANES spectrum are indicated as gray circles. The other axial bond lengths considered in Figure S9 are indicated as gray ×'s. The rhodibalamin ring was used for the excited state.

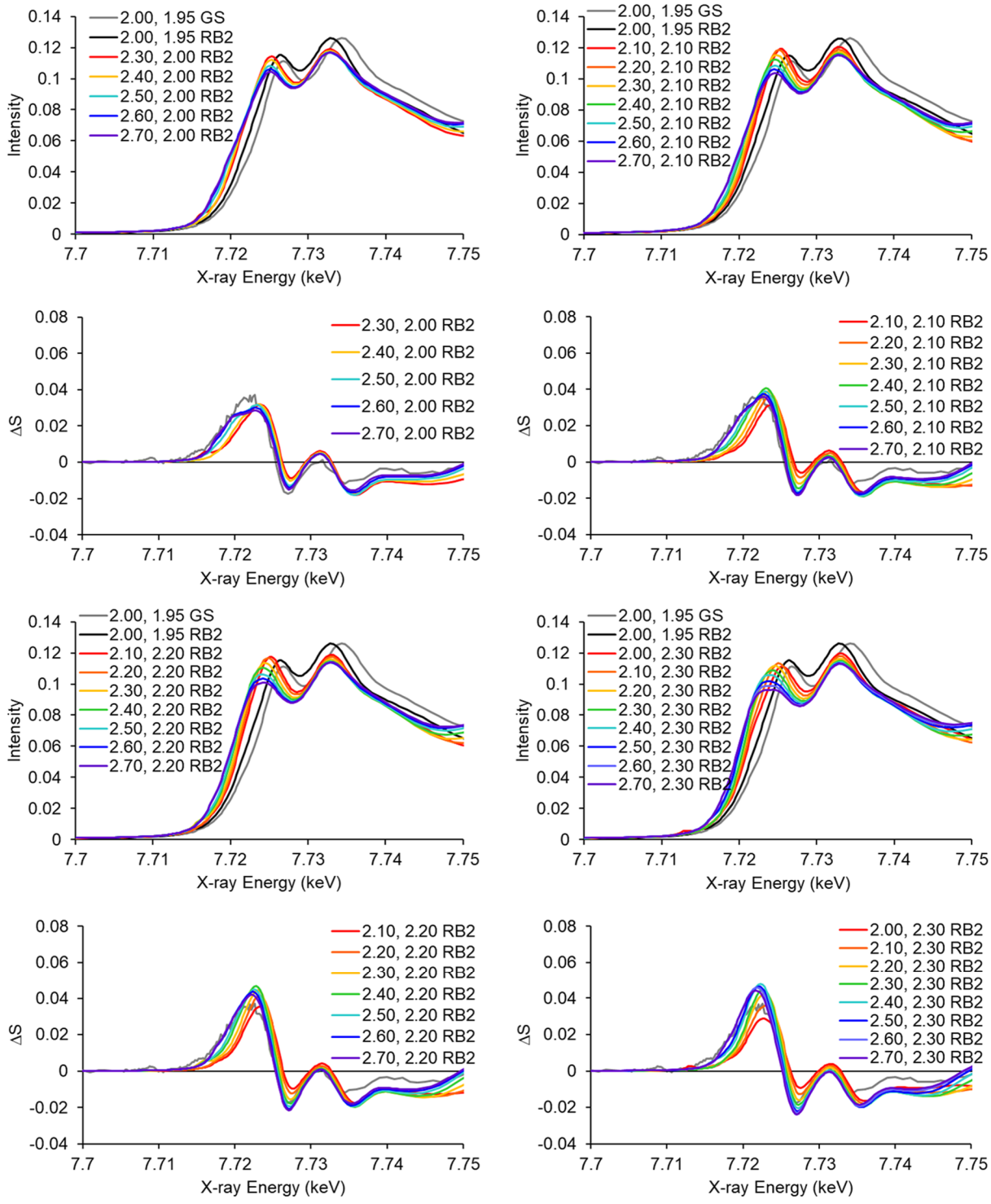

Figure S15a. Trends in the XANES spectrum following changes in the Co-N_{DMB} bond length for set values of the Co-O bond length. The lower panels compare the difference spectra with the experimental result (gray line) for H_2OCbl^+.

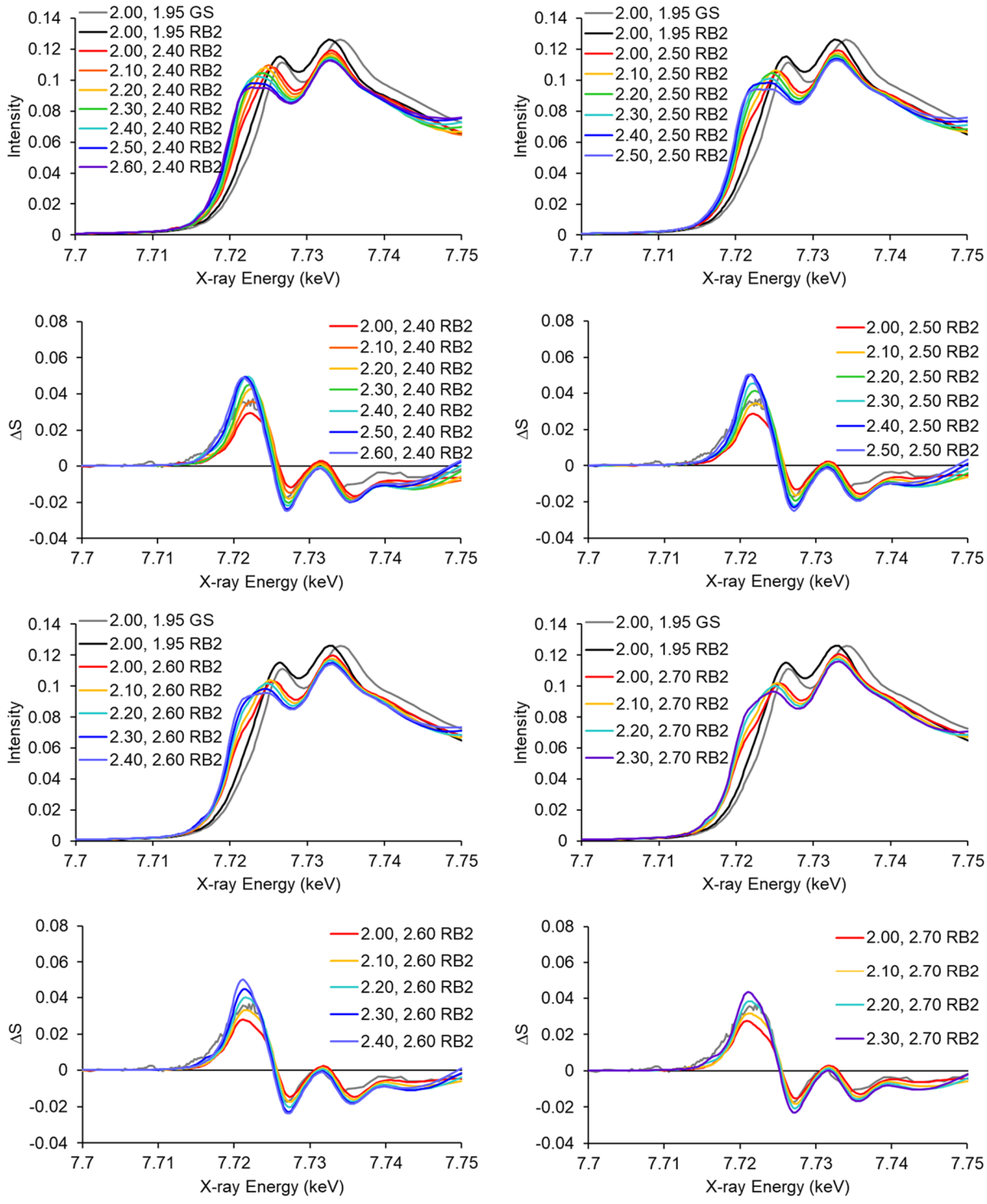

Figure S15b. Trends in the XANES spectrum following changes in the Co-N_{DMB} bond length for set values of the Co-O bond length. The lower panel in each pair compares the difference spectra with the experimental result assuming the excitation fraction $f = 0.4$ (gray line).

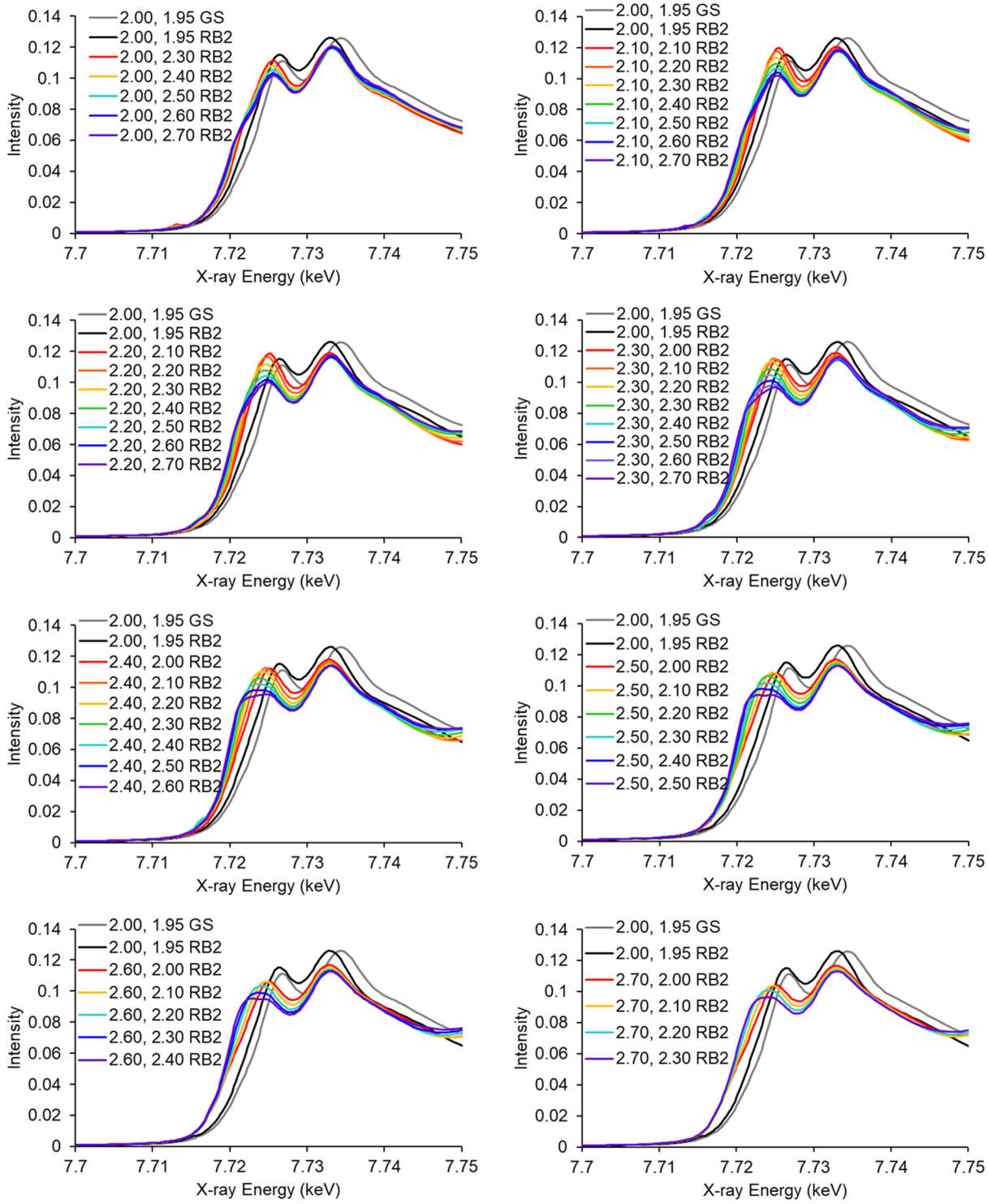

Figure S15c. Trends in the XANES spectrum following changes in the Co-O bond length for set values of the Co-N_{DMB} bond length.

FDMNES Simulations of Species at t>500 fs (C)

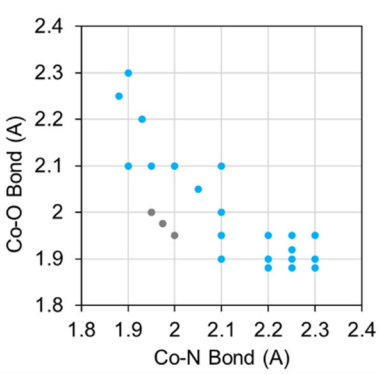

Figure S16. FDMNES simulations were performed for the axial bond lengths indicated in blue on this grid. The ground state structure was used for the corrin ring. The ground state bond lengths consistent with the measured XANES spectrum are indicated in gray. As described above, these yield nearly identical spectra. The difference spectra are between the spectrum with changes in the axial bonds and the ground state spectrum.

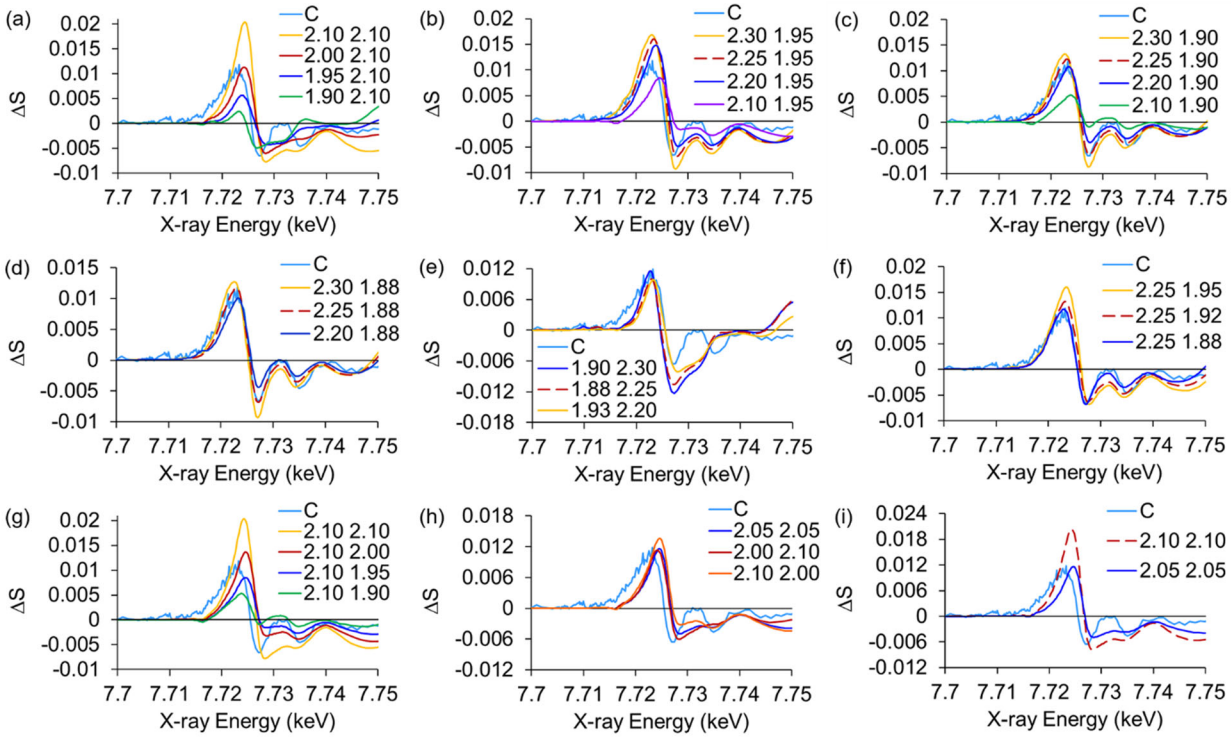

Figure S17. Isotropic difference spectra calculated for the indicated axial bond lengths (Co-N_{DMB}, Co-O in Å) and compared with the experimental spectrum of C. Panels (a)-(d) compare the results holding the Co-O distance constant and varying the Co-N_{DMB} distance. The best agreement is found for Co-N_{DMB} ca. 2.2 to 2.3 Å and Co-O ca. 1.88 to 1.90 Å. Panel (e) compares the results if the Co-N_{DMB} is contracted and the Co-O expanded. Panel (f) and (g) compare the results holding the Co-N_{DMB} distance constant and varying the Co-O distance. Panels (h) and (i) make other comparisons.

Influence of Axial Bonds on the Valence-to-Core Emission and Pre-Edge Absorption.

The hypothesis that the species **C** is a "hot" conformation on the ground electronic state, rather than an electronic excited state, was tested for both H_2OCbl^+ and HOCbl by calculating the valence-to-core emission of each molecule and the pre-edge transitions of H_2OCbl^+ using the axial bond lengths deduced from the XANES measurements. These calculations assume a ground state electronic configuration for the molecule prior to X-ray absorption. The valence-to-core emission results are plotted in Figure S18. While much of the difference at energies >7.706 keV can be accounted for by axial distortion in the ground electronic state, the decrease in emission as ca. 7.707 keV is not reproduced in the simulation. This is consistent with the observation that the dominant transitions in this region are confined to the ring, with relatively little involvement of the axial ligands.

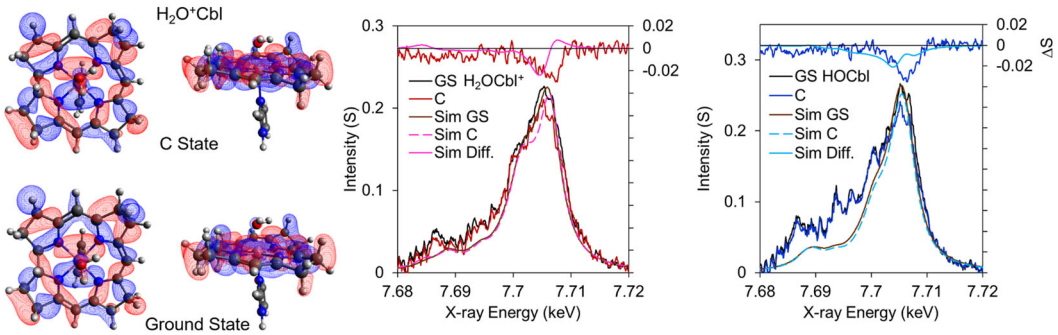

Figure S18. Comparison of the ground and excited **C** state valence-to-core emission with simulations of the ground state emission using structures consistent with the XANES measurements for both states. The change in the axial bond lengths alone is not sufficient to account for the decrease in emission at the peak of the spectrum (ca. 7.707 keV). The orbitals contributing to the dominant transition of H_2OCbl^+ at ca. 7.7062 eV are pictured to the left. These are confined to the ring with little involvement of the axial ligands.

Sample FDNMES input file

```
! Indata file for the fdmnes program
! Use the TDDFT formalism, edge K.

Filout
./rec_1975-1975.txt

Range
-25.  1  0. 0.25 20. 0.5 30. 1. 40.

Radius
8

Density
SCF
Quadrupole

Edge
K

Polarize
1.0 0.0 0.0  0.0 0.0 1.0
0.0 1.0 0.0  0.0 0.0 1.0
0.0 0.0 1.0  1.0 1.0 0.0

Pdb_file
./Rec_1975-1975.pdb

Convolution      !keywords for the convolution
Efermi
-3.5
Estart
-16.
Gamma_max
5.5
Ecent
30.


End
```

Rec_1975-1975.pdb Structure:

```
Co   0.000   0.000   0.000
N   -1.249  -1.404  -0.085
N   -1.400   1.270   0.156
```

N	1.409	1.278	0.062
N	1.239	-1.413	0.054
C	-0.704	-2.766	-0.353
C	-1.854	-3.688	0.198
C	-3.096	-2.777	0.013
H	-3.795	-2.969	0.827
C	-2.502	-1.405	0.203
C	-3.207	-0.248	0.709
C	-2.671	0.988	0.657
C	-3.253	2.313	1.165
C	-2.521	3.303	0.229
H	-2.369	4.255	0.737
C	-1.215	2.585	0.078
C	0.000	3.219	0.000
H	-0.008	4.301	-0.130
C	1.223	2.602	0.071
C	2.523	3.342	0.279
C	3.520	2.285	-0.224
H	4.421	2.298	0.390
C	2.764	0.994	-0.007
C	3.332	-0.245	0.000
C	2.528	-1.436	0.088
C	3.032	-2.844	0.398
C	1.769	-3.684	0.102
H	1.752	-3.880	-0.970
C	0.641	-2.716	0.403
H	0.441	-2.735	1.474
C	-0.443	-2.960	-1.845
H	-0.184	-4.002	-2.036
H	0.382	-2.319	-2.157
H	-1.339	-2.699	-2.408
C	-1.934	-5.035	-0.513
H	-1.995	-4.876	-1.590
H	-2.820	-5.572	-0.175
H	-1.044	-5.621	-0.285
C	-1.704	-3.931	1.709
H	-0.718	-4.348	1.915
H	-1.759	-2.971	2.223
H	-2.470	-4.630	2.043
C	-3.842	-2.926	-1.322
H	-3.201	-2.591	-2.137
H	-4.108	-3.972	-1.476
H	-4.750	-2.323	-1.302
C	-4.496	-0.520	1.440
H	-4.511	-1.556	1.777

H	-5.338	-0.346	0.770
H	-4.572	0.145	2.301
C	-4.757	2.503	1.148
H	-5.199	1.976	1.994
H	-5.163	2.107	0.217
H	-4.991	3.565	1.219
C	-2.681	2.598	2.581
H	-1.624	2.852	2.502
H	-3.187	3.477	2.980
H	-2.798	1.713	3.206
C	-3.217	3.528	-1.105
H	-3.503	2.567	-1.533
H	-4.131	4.098	-0.938
H	-2.540	4.043	-1.786
C	2.690	3.507	1.799
H	2.743	2.524	2.268
H	1.839	4.056	2.201
H	3.608	4.056	2.006
C	2.574	4.694	-0.396
H	3.558	5.139	-0.248
H	1.814	5.344	0.038
H	2.385	4.577	-1.463
C	3.891	2.377	-1.696
H	3.023	2.702	-2.270
H	4.217	1.399	-2.050
H	4.701	3.095	-1.822
C	4.824	-0.359	-0.049
H	5.119	-0.890	-0.954
H	5.175	-0.907	0.826
H	5.263	0.639	-0.052
C	3.392	-2.831	1.894
H	3.803	-3.800	2.178
H	2.496	-2.631	2.482
H	4.132	-2.053	2.083
C	4.217	-3.390	-0.411
H	5.120	-2.838	-0.151
H	4.384	-4.427	-0.121
H	4.014	-3.275	-1.476
C	1.754	-5.034	0.810
H	2.699	-5.181	1.333
H	0.934	-5.060	1.527
H	1.618	-5.829	0.076
N	0.023	0.186	-1.966
C	1.151	0.141	-2.650
H	2.118	-0.100	-2.209

```
N    0.968   0.420  -3.938
H    1.702   0.475  -4.658
C   -2.350   0.563  -2.778
H   -2.843   0.388  -1.821
C   -3.090   0.888  -3.895
H   -4.175   0.972  -3.820
C   -2.448   1.125  -5.139
H   -3.038   1.423  -6.006
C   -1.105   0.971  -5.257
H   -0.610   1.108  -6.218
C   -0.378   0.637  -4.131
C   -0.971   0.462  -2.887
O   -0.019  -0.147   1.969
H   -0.784  -0.140   2.536
H    0.803   0.087   2.389
```

Sample ORCA input file

XES

```
%pal nprocs 6 end
! UKS B3LYP ZORA-def2-TZVP def2/J RIJCOSX TightSCF Grid4 ZORA
! NoFinalGrid Largeprint

%basis newGTO Co "CP(PPP)" end
end

%method SpecialGridAtoms 27
    SpecialGridIntAcc 7
    end

%xes CoreOrb 0,0
  OrbOp 0,1
  end

* xyzfile 2 1 OH2Cbl.xyz
```

XAS

```
%pal nprocs 6 end
! RKS B3LYP TIghtSCF ZORA-def2-TZVP
! SARC/J D3BJ RIJCOSX Grid5 ZORA
! PAL6 Largeprint
%maxcore 5000
%method SpecialGridAtoms 27
```

```
      SpecialGridIntAcc 7
      end

  %tddft
    NRoots 200
    MaxDim 100
    Orbwin[0] = 0,0,-1,-1
    Doquad true
    end

  * xyzfile 2 1 OH2Cbl.xyz
```

OH2Cbl.xyz Truncated Structure

```
Co       0.000   0.000   0.000
N       -1.249  -1.404  -0.085
N       -1.400   1.270   0.156
N        1.409   1.278   0.062
N        1.239  -1.413   0.054
C       -0.704  -2.766  -0.353
H       -0.604  -2.913  -1.428
C       -1.854  -3.688   0.198
H       -1.950  -4.568  -0.437
H       -1.694  -3.874   1.260
C       -3.096  -2.777   0.013
H       -3.795  -2.969   0.827
H       -3.470  -2.874  -1.006
C       -2.502  -1.405   0.203
C       -3.207  -0.248   0.709
H       -4.194  -0.380   1.152
C       -2.671   0.988   0.657
C       -3.253   2.313   1.165
H       -2.933   2.480   2.194
H       -4.323   2.342   0.960
C       -2.521   3.303   0.229
H       -2.369   4.255   0.737
H       -3.031   3.338  -0.734
C       -1.215   2.585   0.078
C        0.000   3.219   0.000
H       -0.008   4.301  -0.130
C        1.223   2.602   0.071
C        2.523   3.342   0.279
H        2.555   4.213  -0.376
H        2.678   3.511   1.345
C        3.520   2.285  -0.224
H        4.421   2.298   0.390
```

H	3.696	2.429	-1.290
C	2.764	0.994	-0.007
C	3.332	-0.245	0.000
H	4.417	-0.335	-0.053
C	2.528	-1.436	0.088
C	3.032	-2.844	0.398
H	3.278	-2.918	1.457
H	3.820	-3.111	-0.306
C	1.769	-3.684	0.102
H	1.752	-3.880	-0.970
H	1.721	-4.525	0.794
C	0.641	-2.716	0.403
H	0.441	-2.735	1.474
N	0.023	0.186	-1.966
C	1.151	0.141	-2.650
H	2.118	-0.100	-2.209
N	0.968	0.420	-3.938
H	1.702	0.475	-4.658
C	-0.971	0.462	-2.887
H	-2.055	0.541	-2.801
C	-0.378	0.637	-4.131
H	-0.952	0.900	-5.020
O	-0.019	-0.147	1.969
H	0.875	-0.006	2.264
H	-0.408	0.679	2.239

Data Availability

Data are available at https://deepblue.lib.umich.edu/